

UC Irvine

UC Irvine Previously Published Works

Title

Highly nonlinear photoluminescence threshold in porous silicon

Permalink

<https://escholarship.org/uc/item/8d52b68p>

Journal

Applied Physics Letters, 75(26)

ISSN

0003-6951

Authors

Nayfeh, M
Akcakir, O
Therrien, J
[et al.](#)

Publication Date

1999-12-27

DOI

10.1063/1.125553

Copyright Information

This work is made available under the terms of a Creative Commons Attribution License, available at <https://creativecommons.org/licenses/by/4.0/>

Peer reviewed

Highly nonlinear photoluminescence threshold in porous silicon

M. Nayfeh,^{a)} O. Akcakir, J. Therrien, Z. Yamani,^{b)} N. Barry, W. Yu, and E. Gratton
Department of Physics, University of Illinois at Urbana-Champaign, Urbana, Illinois 61801

(Received 13 July 1999; accepted for publication 4 November 1999)

Porous silicon is excited using near-infrared femtosecond pulsed and continuous wave radiation at an average intensity of $\sim 10^6$ W/cm² (8×10^{10} W/cm² peak intensity in pulsed mode). Our results demonstrate the presence of micron-size regions for which the intensity of the photoluminescence has a highly nonlinear threshold, rising by several orders of magnitude near this incident intensity for both the pulsed and continuous wave cases. These results are discussed in terms of stimulated emission from quantum confinement engineered intrinsic Si-Si radiative traps in ultrasmall nanocrystallites, populated following two-photon absorption. © 1999 American Institute of Physics. [S0003-6951(99)04852-4]

The discovery in 1990 of strong visible red luminescence by Canham^{1,2} in electrochemically etched silicon surprised the scientific community since silicon is an indirect gap material. It is now believed that the basic mechanism is based on quantum confinement and that the material is made of interconnected Si nanocrystallites (quantum dots) or nanowires.^{1,2} But there is no agreement to whether the basic mechanism is radiative recombination of free excitons in the core or recombination via surface radiative traps. Although there has been interest in the nonlinear optical response of the material³ under a variety of multiphoton infrared excitation including 1.06, 1.3, and 4.9 μm radiation, requiring 3, 3, and 15 photon processes to achieve direct gap excitation of carriers, the interest has been dampened by the fact that the luminescence is wide band and of low quantum efficiency. In this work, we examine some aspects of the nonlinear regime using two-photon femtosecond pulsed and continuous wave (cw) near-infrared excitation with much higher intensities whereby appreciable excitation is induced. We demonstrate a surprising effect of a highly nonlinear photoluminescence threshold in both hydrogen passivated and oxygen passivated samples. Our results demonstrate the presence of micron-size regions for which the intensity of the photoluminescence rises by several orders of magnitude near an average incident intensity of 8×10^5 W/cm² (7×10^{10} W/cm² peak intensity) under both pulsed femto second and cw excitation. It was observed that in contrast to most of the surface, those regions do not luminesce in the red under ultraviolet (365 nm) excitation. The results are discussed in terms of stimulated emission from quantum confinement-engineered intrinsic Si-Si radiative traps in ultrasmall nanocrystallites, populated following two-photon absorption.

The samples were (100) oriented, 1–10 Ω cm resistivity, *p*-type boron doped silicon wafers, laterally anodized in a solution of hydrogen peroxide and hydrofluoric acid, using current densities in the range 20–130 mA/cm².⁴ The substrate acted as the anode and a platinum wire acted as a cathode. High quality oxidation is achieved by immersion in a H₂O₂ bath. We used cw and mode locked femtosecond

Ti-sapphire near infrared laser system, generating pulses of 150 fs duration at a repetition rate of 80 MHz. At the target, the average power, 5–20 mW, is focused to a spot of 2 μm diameter using a 0.4 numerical aperture lens, giving a peak pulse intensity of 10^{11} W/cm² at the high end of this range, with a corresponding cw beam intensity of 10^6 W/cm². The beam-sample interaction region is viewed via an optical microscope ($\times 20$) and the excitation light was raster scanned over a region of interest allowing photoluminescence imaging. The incident intensity was varied by neutral density filters. Emission is detected by a photomultiplier and stored in a two-dimensional array.

Figure 1 shows two luminescence images of a $132 \times 132 \mu\text{m}$ section of a hydrogen passivated sample under femtosecond pulsed illumination at increasing intensity (the color in the images is not the color of the emission). Figure 1(a) is taken at an average incident intensity of 5.7×10^6 W/cm² (5×10^{10} W/cm² peak intensity) and 780 nm wavelength. The image shows a surface broken up into irregular weakly luminescent (observed orange/red by naked eye) islands of a few micrometers across. This topography of islands is reproduced in electron scanning microscopy. Figure 1(b) is taken at an average intensity of 8×10^5 W/cm²; it shows numerous, extremely bright greenish spots (observed by naked eye) within the islands, while most of the surface is weakly luminescent (in the orange/red). We also imaged samples that have been passivated with a high quality oxide by immersion in hydrogen peroxide, showing similar effects as a function of incident intensities. Hydrogen was substituted by an ultrathin high quality oxygen coating (1 mL)^{5,6} by immersion in hydrogen peroxide, with a trap density of less than $1/10^{14}$.⁷

Figure 2 gives the emission intensity for several individual bright spots as a function of the average incident intensity under pulsed illumination. Across a threshold of $\sim 5 \times 10^5$ W/cm², it rises by several orders of magnitude. From the log-log inset, we see a dramatic increase in the slope of the power pumping curve from ~ 1.6 to ~ 11 – 12 . In regions clear of the bright areas, however, the power dependence remains at ~ 1.6 above this threshold intensity. Moreover, for intensity lower than $\sim 5 \times 10^5$ W/cm², the power dependence is 1.9–2. Measurements were also made by tar-

^{a)}Electronic mail: m-nayfeh@uiuc.edu

^{b)}Permanent address: KFUPM, Dhahran, Saudi Arabia.

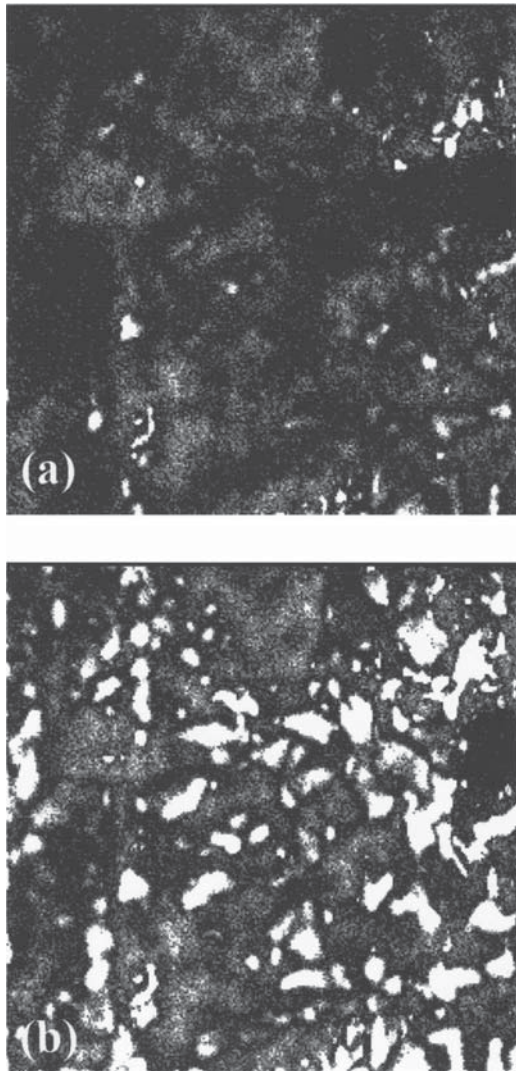


FIG. 1. A $132 \times 132 \mu\text{m}$ luminescent images of a hydrogen passivated material, under femtosecond pulsed excitation. The laser spot is raster scanned across the sample while its average intensity is kept at the same level: (a) at 5.7×10^5 and (b) at $8 \times 10^5 \text{ W/cm}^2$. The surface shows numerous, extremely bright spots at the high intensity.

getting individual brighter spots and varying the incident intensity using neutral density filters.

Operating the laser in cw mode provides a beam of power equal to the average power in the pulsed case and focused to the same excitation spot size via the same objec-

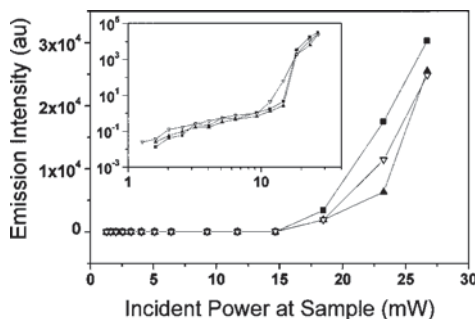


FIG. 2. The emission intensity under femtosecond pulsed excitation as a function of the average power of the incident radiation for several individual micron size bright spots. The inset is the log-log of the data with the same axis labels. An average power of 15 mW corresponds to an average intensity of $5 \times 10^5 \text{ W/cm}^2$.

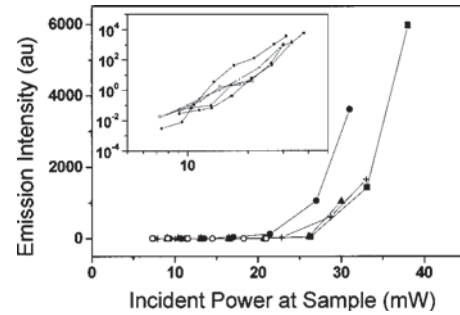


FIG. 3. Integrated emission intensity of a $132 \times 132 \mu\text{m}$ section as a function of cw incident intensity, with the same beam geometry as in the pulsed case. An average power of 30 mW corresponds to an average intensity of 10^6 W/cm^2 . The inset is log-log of the data with the same axis labels. \circ 900, $+$ 870, \blacksquare 830 \blacktriangle 800, and \bullet 790 nm.

tive. The bulk of the surface shows no orange/red luminescence under cw illumination up to 80 mW incident power. This is unlike the pulsed case where, at 10 mW average power, the bulk of the surface is luminescent orange/red. At $\sim 20 \text{ mW}$ cw incident power, the bright greenish luminescent spots turn on comparable to the pulsed case. The integrated luminescence emission curves as a function of pump power from the scan in an $132 \times 132 \mu\text{m}$ section, given in Fig. 3, shows that the threshold occurs at an intensity of $6.4 \times 10^5 \text{ W/cm}^2$ ($\sim 20 \text{ mW}$ average power), somewhat higher than the average intensity needed in the pulsed case ($5 \times 10^5 \text{ W/cm}^2$ average power). The log-log inset gives a large slope above threshold (\sim ten), similar to the pulsed case. Thus, the brightest spots distinguished by the color of their emission have somewhat similar characteristics (threshold and power dependence) under femtosecond pulsed or cw excitation. The excitation spectra (emission multiplied by absorption) were recorded under cw excitation as a function of the incident wavelength in the range 720–860 nm. The spectra (not presented here), taken at a constant incident power of 50 mW ($1.6 \times 10^6 \text{ W/cm}^2$), well above the reported threshold, show a trend of increasing emission with decreasing wavelength.

We note that the brighter spots are found in regions where the anodizing current concentrates, such as in the meniscus (air-liquid interface) or at the sharp edges or points of surface steps or grooves. Grooves or scratches may be fabricated at controlled locations on the sample prior to anodization. Our previous studies showed that higher current density catalyzes etching rates, resulting in smaller substructure.^{8,9} Thus, it appears that it is the smallest structures in these regions that respond strongly to the pulsed radiation as well as to the cw excitation. On the other hand, it is the larger ones, which constitute most of the material, that respond moderately to the pulsed radiation, and negligibly to the cw excitation.

We now speculate on the origin of the process. We believe it is not a high order multiphoton absorption process (of order 10–12) since, at photon energy of 1.56 eV, two to three photon energies are sufficient to induce direct gap absorption. Moreover, our measurements give a low power dependence (sub quadratic) at high but just below a threshold intensity. Thus, we conclude that the high nonlinearity is associated with the emission step, and that it is sensitive to the size of the nanostructures. The large variance in the

power dependence across the narrow intensity range resembles stimulated emission in systems of inverted population. In this regard, there exists a model^{10,11} in which strong variations in the absorption and emission pathways occur with variation in size, especially in the ultrasmall size regime. Allan *et al.*¹⁰ theoretically discovered the formation, in ultrasmall nanocrystallites (<1.75 nm), of a new stable configuration (or phase), distinct from but interconnected to a diamond-like structure by a potential barrier. It is based on the pairing of surface atoms to form intrinsic Si–Si dimer bonds. The excited state interatomic potential (not shown here but may be found in Refs. 10 and 11) is a double well with a potential barrier where the outer well, a trap well, (at 3.85 Å) radiates with life times of tens of 10 μs, while the inner well (at 2.35 Å) is nonradiative, with a much longer radiative time scale (millisecond). The state to which the outer well radiates (at 3.85 Å) is the ground electronic state. But, at this bond length, the vibrational states in the ground state are high lying and unpopulated, hence, this system may constitute a stimulated emission channel. Direct minimum to minimum excitation from the ground state to the outer well is not allowed because transitions proceed vertically according to the Frank–Condon principle. But absorption proceeds into the inner well at bond length of 2.35 Å, followed by transfer into the outer well by bond expansion via tunneling (double well vibrations) or thermal activation.¹¹ Alternatively, above-barrier absorption at higher incident photon energy, followed by relaxation populates the trapping well. For sizes less than a critical size of ~1.4 nm, the trapping edge is lower than the absorption edge, hence, it is thermally stable, allowing strong transfer from the inner well to the radiative well.¹¹ Evidence for Si–Si radiative traps, based on a potential barrier, has been derived in recent experiment from the manipulation by high quality ultrathin oxides or conductors.¹²

To achieve appreciable absorption, at the powers used in the experiment, namely at 5×10^{10} W/cm² peak intensity for the femtosecond excitation (photon flux of 2×10^{29} /cm²s), one needs to induce a transition rate R that compares with the reciprocal of the pulse duration T . For $RT=0.5$, for example, where $T=150$ fs, $R=4 \times 10^{12}$ /s. This requires a two-photon absorption “cross section” $\beta \sim 10^{-46}$ cm⁴s, with an absorption rate $R = \beta F^2$ where F is the number of incident photons/cm²s. A cross section of this magnitude is not totally unrealistic. A 30 mW continuous wave excitation beam, on the other hand, focuses to $\sim 1 \times 10^6$ W/cm² (photon flux of 4×10^{24} /cm²s), which gives a corresponding absorption rate of 10^3 /s, down by several orders of magnitude from the pulsed case, but large enough to produce significant probabilities within tens of microseconds, the emission lifetime. We note that at a repetition rate of 80 MHz, the emission lifetime is much longer than the laser duty cycle (12 ns), thus accumulation of population may be taking place. But the transfer of the population to the outer well trap may only proceed strongly in ultrasmall nanostructures.^{10,11} Although there is an analytical theory for a single photon absorption in nanocrystallites,¹³ there are no calculations for two-photon cross sections.

It is to be noted that there were several advances over previous measurements³ that contributed to the observations

we are reporting. First, unlike previous methods, our distinct anodization procedure produces much smaller substructures, accessing the regime of ultrasmall nanostructure where interesting size effects take place.^{8,9} This is accomplished by incorporating a highly catalyzing H₂O₂ chemical,⁴ and by utilizing lateral electrode configuration to concentrate the anodization current to the very top skin of the wafer, and onto surface discontinuities. Second, the procedure provides high chemical and electronic qualities, brought about by the incorporation of the highly cleansing hydrogen peroxide in the etchant.⁴ Such superior properties allow the use of low order radiative processes for direct carrier excitation (two-photon near-infrared excitation) without incurring damage to the sample. Finally, using spatially resolved photoluminescence imaging with submicrometer resolution allows us to attain high intensities while resolving small regions that otherwise would be averaged out when using excitation beams of large cross sections and/or low intensity.

In conclusion, two-photon excitation of porous silicon demonstrates a highly nonlinear threshold in which the visible emission intensity rises by several orders of magnitude over a narrow range of incident intensity under either femtosecond or cw near-infrared excitation. The large variance in the power dependence resembles stimulated emission in systems of inverted population. These results are not only important because of the potential for integration of microstimulated emission systems in silicon chips, but because the results may contribute to the elucidation of the basic mechanism for the optical activity of porous silicon.

The authors gratefully acknowledge the U.S. Department of Energy (Grant No. DEFG02-91-ER45439), the National Institute of Health (RR03155), and the University of Illinois at Urbana-Champaign.

- ¹L. T. Canham, *Appl. Phys. Lett.* **57**, 1046 (1990).
- ²See for example: A. G. Cullis, L. T. Canham, and P. Calcott, *J. Appl. Phys.* **82**, 909 (1997).
- ³J. Wang, H.-B. Jiang, W.-C. Wang, J.-B. Zheng, F.-L. Zhang, P.-H. Hao, X.-Y. Hou, and X. Wang, *Phys. Rev. Lett.* **69**, 3252 (1992); J. Gole and D. Dixon, *J. Appl. Phys.* **83**, 5985 (1998); F. Koch, *Mater. Res. Soc. Symp. Proc.* **298**, 222 (1993); R. P. Chen, Y. R. Shen, and V. Petrova-Koch, *Science* **270**, 776 (1995).
- ⁴Z. Yamani, H. Thompson, L. AbuHassan, and M. H. Nayfeh, *Appl. Phys. Lett.* **70**, 3404 (1997); D. Andsager, J. Hilliard, J. M. Hetrick, L. H. AbuHassan, M. Plisch, and M. H. Nayfeh, *J. Appl. Phys.* **74**, 4783 (1993).
- ⁵W. H. Thompson, Z. Yamani, L. Abuhassan, O. Gurdal, and M. Nayfeh, *Appl. Phys. Lett.* **73**, 841 (1998); W. H. Thompson, Z. Yamani, L. Abuhassan, J. Green, M. Alhassan, and M. Nayfeh, *J. Appl. Phys.* **80**, 5415 (1996).
- ⁶S. I. Raider, R. Flitsch, and M. J. Palmer, *J. Electrochem. Soc.* **122**, 413 (1975); U. Neuwald, A. Feltz, U. Memmert, and R. J. Behm, *J. Appl. Phys.* **78**, 4131 (1995).
- ⁷A. Pasquarello, M. S. Hybertsen, and R. Car, *Phys. Rev. Lett.* **74**, 1024 (1995).
- ⁸Z. Yamani, S. Ashhab, A. Nayfeh, and M. H. Nayfeh, *J. Appl. Phys.* **83**, 3929 (1998).
- ⁹Z. Yamani, N. Rigakis, and M. H. Nayfeh, *Appl. Phys. Lett.* **72**, 2556 (1998); Z. Yamani, O. Gurdal, A. Alaql, and M. Nayfeh, *J. Appl. Phys.* **85**, 8050 (1999).
- ¹⁰G. Allan, C. Delerue, and M. Lannoo, *Phys. Rev. Lett.* **76**, 2961 (1996).
- ¹¹M. Nayfeh, N. Rigakis, and Z. Yamani, *Phys. Rev. B* **56**, 2079 (1997); *Mater. Res. Soc. Symp. Proc.* **486**, 243 (1998).
- ¹²Z. Yamani, A. Alaql, J. Therrien, O. Nayfeh, and M. H. Nayfeh, *Appl. Phys. Lett.* **74**, 3483 (1999).
- ¹³E. Hanamura, *Phys. Rev. B* **37**, 1273 (1988).